CRYSTALLOCHEMICAL CHARACTERIZATION OF THE PALYGORSKITE AND SEPIOLITE FROM THE ALLOU KAGNE DEPOSIT, SENEGAL

E. García-Romero[1,*], M. Suárez[2], J. Santarén[3] and A. Alvarez[3]

[1] Departamento de Cristalografía y Mineralogía, Universidad Complutense de Madrid, E-28040 Madrid, Spain
[2] Departamento de Geología, Universidad de Salamanca, E-37008 Salamanca, Spain
[3] TOLSA Ctra Vallecas-Mejorada del Campo, km 1600, 28031 Madrid, Spain

Abstract—The Allou Kagne (Senegal) deposit consists of different proportions of palygorskite and sepiolite, and these are associated with small quantities of quartz and X-ray amorphous silica as impurities. No pure palygorskite or sepiolite has been recognized by X-ray diffraction. Textural and microtextural features indicate that fibrous clay minerals of the Allou Kagne deposit were formed by direct precipitation from solution. Crystal-chemistry data obtained by analytical/transmission electron microscopy (AEM/TEM) analyses of isolated fibers show that the chemical composition of the particles varies over a wide range, from a composition corresponding to palygorskite to a composition intermediate between that of sepiolite and palygorskite, but particles with a composition corresponding to sepiolite have not been found. Taking into account the results from selected area electron diffraction and AEM-TEM, fibers of pure palygorskite and sepiolite have been found but it cannot be confirmed that all of the particles analyzed correspond to pure palygorskite or pure sepiolite because both minerals can occur together at the crystallite scale. In addition, the presence of Mg-rich palygorskite and very Al-rich sepiolite can be deduced.

It is infrequent in nature that palygorskite and sepiolite appear together because the conditions for simultaneous formation of the two minerals are very restricted. The chemical composition of the solution controls the formation of the Allou Kagne sepiolite and palygorskite. The wide compositional variation appears as a consequence of temporary variations of the chemical composition of the solution.

Key Words—AEM-TEM, Allou-Kagne Deposits, Crystal Chemistry, Palygorskite, SAED, Senegal, Sepiolite.

INTRODUCTION

Sepiolite and palygorskite are fibrous clay minerals with many industrial applications due to their structural and physicochemical properties. They are used as absorbents and as adsorbents (cat litter, separation of gases, filters, *etc.*); they have rheological properties (drilling mud on salt water, pharmacy, paint, cosmetic, *etc.*) and have numerous other uses (Alvarez, 1984; Jones and Galán, 1988).

The structure of both sepiolite and palygorskite contains ribbons of 2:1 phyllosilicates linked by periodic inversion of the apical oxygen of the continuous tetrahedral sheet (every six atoms of Si for sepiolite and every four for palygorskite). Sepiolite is a trioctahedral mineral with eight possible octahedral positions per half unit-cell, and all are occupied. The structural formula of sepiolite is $Si_{12}O_{30}Mg_8(OH)_4(OH_2)_4.nH_2O$ (Brauner and Preisinger, 1956). The octahedral sheet is discontinuous and terminal cations must complete their coordination sphere with water molecules. The number of octahedral positions (per half unit-cell) in palygorskite is five, although it does not seem possible that all can be filled (Serna *et al.*, 1977). In most palygorskites the number of occupied positions ranges from four to five, and only a few cases seem to be completely dioctahedral with the structural formula $Si_8O_{20}Al_2Mg_2(OH)_2(OH_2)_4.4H_2O$ (Bradley, 1940).

Palygorskite and sepiolite form in marine or continental sedimentary environments. Both minerals may be formed by direct precipitation from waters with a large degree of salinity coming from strongly weathered continental areas (Castillo, 1991), and both minerals are frequently associated with lacustrine facies in continental sediments where they form from solutions or by diagenetic transformation (Weaver, 1984; Jones and Galán, 1988; Chahi *et al.*, 1997). Palygorskite is especially common in calcretes related to edaphic processes affecting sediments (Singer and Norrish, 1974; Watts, 1980; Singer, 1984; Verrecchia and Le Coustumer, 1996). Palygorskite and sepiolite can also be formed as direct precipitates or as a replacement product from hydrothermal solutions (Tien, 1973; Haji-Vassiliou and Buffer, 1975; López Galindo *et al.*, 1996; Kamineni *et al.*, 1993; Garcia-Romero *et al.*, 2006). In general, their genesis can be related to transformation processes from previous silicates (Yaalon and Wieder, 1976; Suárez *et al.*, 1994; Torres-Ruiz *et al.*, 1994; Lopez-Galindo *et al.*, 1996) or to direct precipitation from solutions (Singer and Norrish, 1974; Watts, 1976; Estéoule-Choux, 1984).

* E-mail address of corresponding author:
mromero@geo.ucm.es

Palygorskite is more abundant than sepiolite and although the two minerals sometimes appear together this is not often the case. There are few references in the literature in which sepiolite and palygorskite occur in the same or adjacent localities. For example, they are described together in the following Spanish deposits: Tajo Basin, (Leguey *et al.*, 1995; Galán and Castillo, 1984), Tabladillo (Martín Pozas *et al.*, 1981); Lebrija (Galán and Ferrero, 1982); and also in central and central-southern Tunisia (Zaaboub *et al.*, 2005), in the Serinhisar-Acipayam Basin (Turkey) (Akbulut and Kadir, 2003), and in the deep-sea mid-Atlantic ridge, of hydrothermal origin (Bowles *et al.*, 1971). In the Allou Kagne deposit, sepiolite and palygorskite appear together. This is an important deposit of special clays.

The aim of this work is the mineralogical and crystallochemical characterization of the palygorskite and sepiolite from the Allou Kagne deposit. The relationships between the two minerals have been studied, both from genetic and compositional viewpoints.

MATERIALS AND METHODS

Materials

The palygorskite and sepiolite studied were obtained from the Allou Kagne (Senegal) deposit which is located ~10 km from the town of Thiès on the road from Dakar to Thiès (Figure 1). This deposit has been known since the second half of the 20th century. Millot (1970) reported it and other deposits of fibrous clays in this region to be of minor economic interest. It is located in the Senegal-Mauritania basin and its genesis is related to sedimentation in an epicontinental marine environment during the Paleogene.

Figure 1. Map of Senegal, showing the Allou-Kagne deposit.

Palygorskite and sepiolite usually appear in horizontal layers, interbedded with carbonates (calcite and dolomite) and, in some cases, accessory minerals like quartz and opal A. The fibrous clay layers typically consist mainly of palygorskite intermingled with variable minor quantities of sepiolite, are of Lower Eocene age, and appear over Paleocene karstified limestones (Figure 2). The bottom of the deposit consists of glauconitic sands containing phosphate and carbonate. The section rich in palygorskite and minor sepiolite is divided into two different zones, the lower being the richest in carbonates (<30%) and containing massive layers, ochre in color, up to 8 m thick. The upper zone of the mineralized section is the purest in terms of content of clay minerals. Parallel laminations in the clay levels are white or beige, and show black and orange spots. In some places, silicified levels are intercalated. The total thickness is rarely >20 m. Between both zones, a thin level of sandstone may appear. This level is ~10 cm thick, is silicified and carbonated, and is a guide level. Samples coming from the upper-zone level were chosen

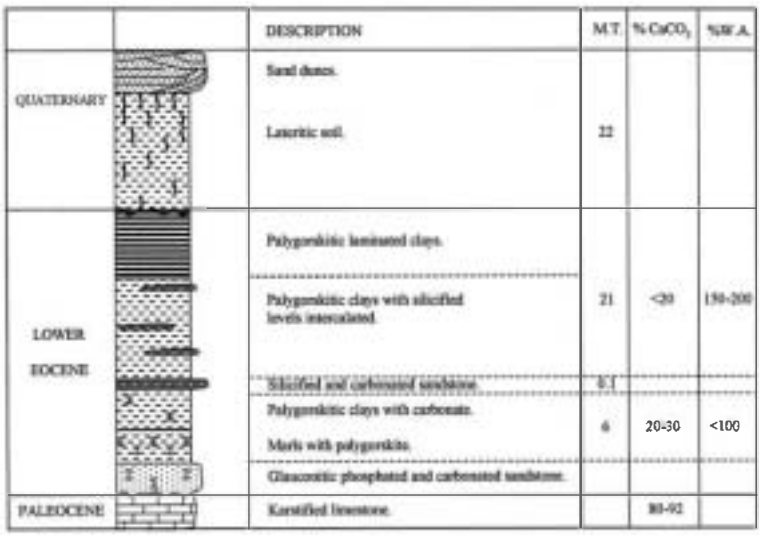

Figure 2. Schematic stratigraphic section of the Allou-Kagne deposit. M.T. – maximum thickness (m). W.A. – water absorption.

for this mineralogical and crystallochemical study. The clay beds of economic interest range from 4 to 20 m thick, with overburden that varies from 0 to 20 m. The proven reserves of the deposit are 25 Mt with inferred resources of >60 Mt.

To the north of the area studied, in which the lithological series is more complete, sediments from Upper Eocene and Oligocene or Mio-Pliocene appear over the palygorskite section. These sediments are composed mainly of phosphated sediments that have formed major deposits of phosphates which are currently mined.

Quaternary silica sands and laterites, and in some cases marly or clayish soil, appear at the top. In the Allou Kagne area, the top of the outcrop consists of a lateritic soil that can reach 20 m thick in some places or, only a few meters in others. Three series of vertical faults have caused sub-vertical displacements of the mineralized bed and have determined variations in the composition and the thickness of the Quaternary sediments.

The clay levels studied show parallel lamination as a consequence of sedimentary origin, and hand specimens exhibit a clear planar structure. The sedimentary structure of the samples was taken into account during their study. Thin layers, ~1 mm thick, were separated to study small-scale compositional variations. A mineralogical and crystallochemical characterization of the samples at this scale was also carried out.

Methods

Mineralogical characterization was performed by X-ray diffraction (XRD) using a Siemens D500 XRD diffractometer with CuKα radiation and a graphite monochromator. The samples used were random-powder specimens which were scanned from 2 to 65°2θ at 0.05°2θ/3 s to determine the mineralogical composition. X-ray diffraction patterns from powdered individual and contiguous layers of hand specimens were recorded in order to determine whether sepiolite and palygorskite are concentrated in different layers or whether both minerals always appear together in similar proportions.

Particle morphology and textural relationships were established by scanning electron microscopy (SEM) and transmission electron microscopy (TEM). The observations were performed using a JEOL JSM 6400 microscope, operating at 20 kV and equipped with a Link System energy dispersive X-ray (EDX) microanalyzer. Prior to examination by SEM, freshly fractured surfaces of representative samples were air dried and coated with Au under vacuum. The TEM observations were performed by depositing a drop of diluted suspension on a microscopic grid with collodion. Selected area electron diffraction (SAED) images and chemical composition by analytical electron microscopy (AEM) were obtained by TEM, in pure samples, using a JEOL 2000 FX microscope equipped with a double-tilt sample holder (up to a maximum of ±45°) at an acceleration voltage of 200 kV, with 0.5 mm zeta-axis displacement and 0.31 nm point-to-point resolution. The microscope incorporates an OXFORD ISIS EDX spectrometer (136 eV resolution at 5.39 keV) and has its own software for quantitative analysis. For AEM analyses, four representative samples with intermediate contents of both minerals, all corresponding to the upper zone of the deposit were chosen. One representative sample was separated into six layers, millimeters thick, and the new samples were named from AKA–AKF. As it was found that there is a progressive variation in the relative proportions of clay minerals, from the richest in palygorskite (AKA) to the richest in sepiolite (AKF), the two extreme samples were chosen for the AEM study. Structural formulae were calculated noting that the ideal formula contains 21 and 32 oxygens for palygorskite and sepiolite, respectively, in the dehydrated and dehydroxylated structure per half unit-cell (Bailey, 1980). All the Fe present was considered as Fe^{3+} (owing to the limitation of the technique), but the possible existence of Fe^{2+} cannot be ruled out.

RESULTS

Mineralogical composition

As already stated, raw samples are composed of different proportions of sepiolite and palygorskite, and they have small quantities of quartz and X-ray amorphous silica as impurities. When several layers of a hand specimen have been studied separately, different proportions of sepiolite and palygorskite have been found in each layer, and the proportion of both minerals varies between contiguous planes. Figure 3 shows the XRD patterns of samples corresponding to contiguous planes which are 1 mm thick obtained from a laminar sample 0.5 cm thick. The progressive variation in the percentages of sepiolite and palygorskite can be observed. No pure sepiolite or palygorskite has been found.

Textural and microtextural features

The combined SEM of raw samples and TEM of dispersed samples have confirmed the characteristic fibrous morphology. A morphological and textural study by SEM indicates that samples are composed of fibers oriented according to the lamination, with the axis of the fibers pointing in all directions (Figure 4a), forming well defined planes, corresponding to their depositional origin (Figure 4b). Idiomorphic crystals of apatite can be observed among the fibers. Although sepiolite and palygorskite appear together even at this scale, as indicated by XRD, differences in size or morphological features have not been found, and it is not possible to distinguish the two minerals in these samples by SEM or TEM. The aggregate growth of individual fibers forming planes does not permit measurement of the precise length of these individual crystals, but it is

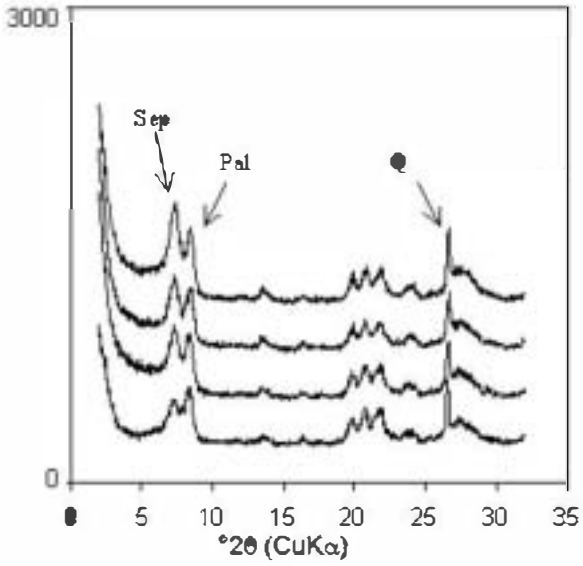

Figure 3. XRD patterns corresponding to contiguous mm-thick layers. Progressive change in the proportions of the two fibrous minerals, sepiolite (Sep) and palygorskite (Pal), can be seen. Q: quartz.

possible to affirm that the fibers are generally >1 μm in length. From a textural point of view, it is possible to observe that the pores are scarce and millimetric in size, because the fibers form planar surfaces and create inter-fiber pores of <100 nm in width.

The characteristic fibrous morphology of both palygorskite and sepiolite can also be observed by TEM. The fibers are >1 μm long (Figure 5c), although size can be influenced by the dispersion procedure which can break the fibers. Groups of fibers are disposed in parallel arrangement forming bundles which correspond to the fibers seen by TEM. When the samples were chosen from different and contiguous layers, no differences in size or morphological features were found.

Likewise, the SAED patterns of elongated bundles of fibers confirmed the close relationship between sepiolite and palygorskite crystals. Although most diffraction patterns of isolated fibers correspond to sepiolite or palygorskite crystals (Figure 5a,b), the same diffraction patterns of sepiolite and palygorskite almost parallel in the same fiber have also been observed. Spots corresponding to reflections of both sepiolite and palygorskite (12 Å and 10.5 Å) appear together, as shown in Figure 5d. This means that both minerals coexist at crystallite scale.

Crystallochemical characterization

Ninety nine TEM point analyses of isolated fibers corresponding to different samples were carried out. The chemical compositions of the particles vary between very wide extremes (Table 1). Samples were selected taking into account the results obtained from XRD study including the richest in palygorskite and sepiolite. In Figure 6, the results obtained for the particles analyzed are plotted together with those corresponding to 'theoretical formulae' of palygorskite and sepiolite. The points are distributed on the graph over a very wide range, from palygorskite to sepiolite composition. There are a few analyses with the ratio SiO_2/MgO and $Al_2O_3+Fe_2O_3$ similar to that corresponding to palygorskite. However, by contrast, no analysis corresponding to a pure sepiolite composition was found.

According to bibliographic references related to the chemical composition of fibrous clay minerals, a compositional gap occurs between the two extremes. The trioctahedral extreme is sepiolite, and the dioctahedral extreme is palygorskite (Martín Vivaldi and Cano, 1956; Paquet *et al.*, 1987; Galán and Carretero, 1999). In this paper, the structural formulae for all analyzed particles were calculated on the basis of both 21

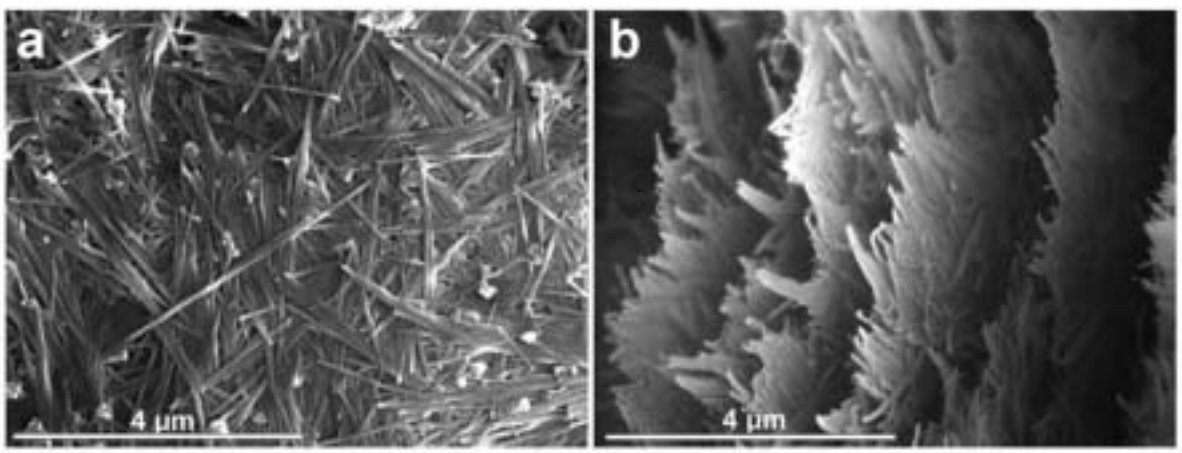

Figure 4. SEM images of the tightened growth of sepiolite-palygorskite fibers forming planes. All fibers are of similar appearance and it is not possible to distinguish sepiolite from palygorskite. (a) Image of a plane of fibers. The axes of the fibers are pointing in all directions and the aggregates form well defined planes. (b) Image of several contiguous planes of fibers. The orientations of the fibers forming the parallellamination is clear.

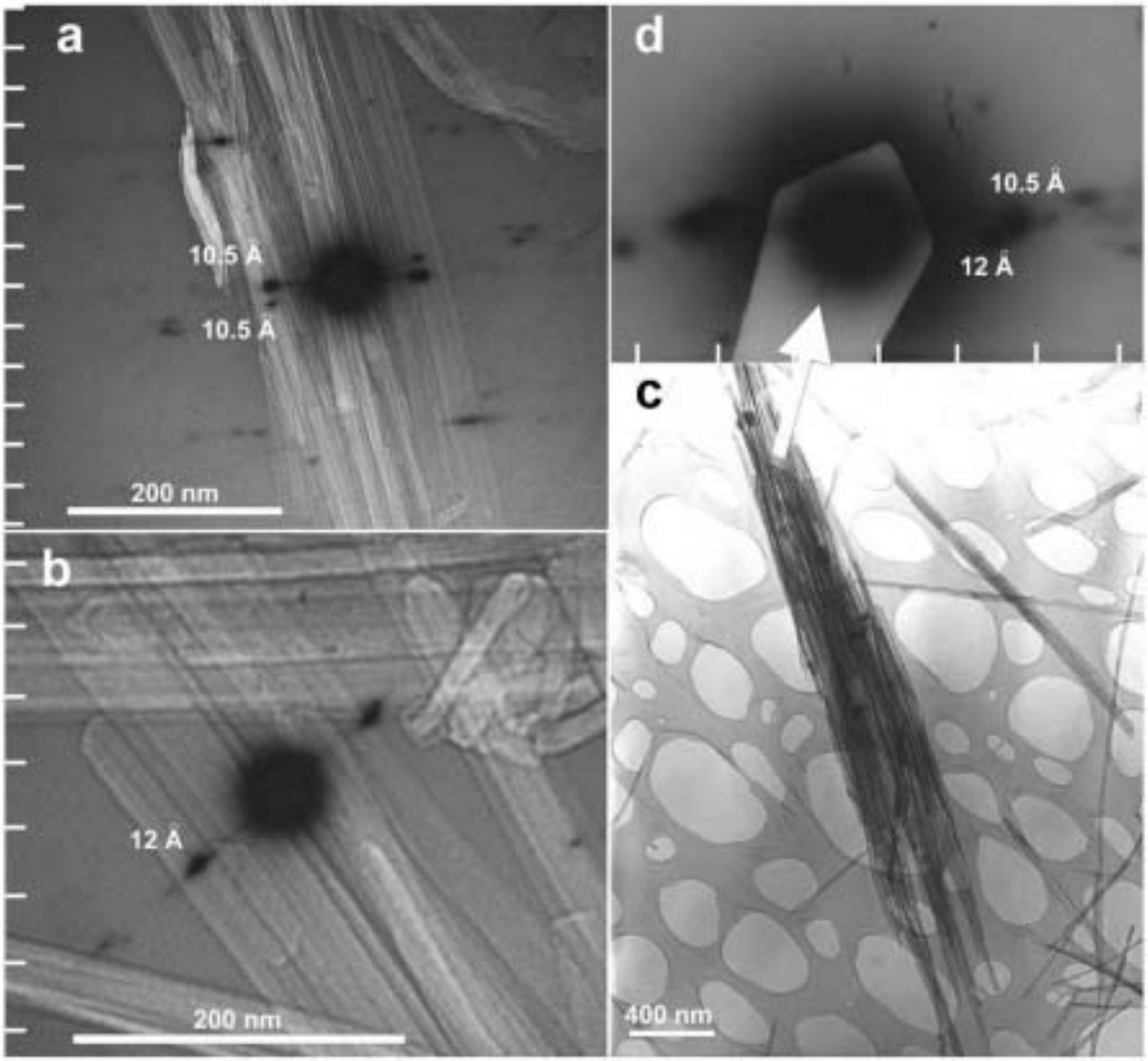

Figure 5. TEM images. (a,b) Superimposed negatives (TEM image and SAED spots) on the image. Camera length (L) – 800 mm, λ – 0.0025 nm. Camera constant (Lλ) – 20.1 in all SAED images. There are two graphic scales: the vertical scale corresponds to the SAED image (1 mm between bars) and the horizontal scale corresponds to the TEM image. (a) There are two 110 electron diffraction spots corresponding to two different bundles of fibers (10.5 Å) of palygorskite which form a small angle, as can be seen in the image of the aggregate. (b) Bundle of fibers of sepiolite and 110 SAED spots from sepiolite fibers (12 Å). (d) Two different 110 SAED spots from sepiolite and palygorskite fibers (10.5 and 12 Å) corresponding to two contiguous fibers that form a small angle in a same bundle. Scale: 1 mm between bars. (c) Bundles of sepiolite palygorskite.

(Table 2) and 32 oxygens per half unit-cell (as palygorskite and sepiolite, respectively) (Table 3) with the aim of separating two groups of analyses (those which fit well either as palygorskite or sepiolite) because it is not possible to identify the two minerals from their morphological features alone. The results obtained show that most of the analyses do not correspond to either pure sepiolite or pure palygorskite. There is no gap between the two groups of formulae, but on the contrary, both groups display a continuous variation. Whether the formulae are fitted as palygorskite or as sepiolite the results are continuous. If palygorskite composition is taken into account (Table 2) there is only a small group of analyses which fit well as palygorskite. Most of the analyses fit with Mg-rich palygorskite, and others are so anomalous that they cannot be considered as palygorskite. However, if sepiolite composition is considered (Table 3) there is no analysis that fits as sepiolite and all analyses should correspond to a very anomalous sepiolite with a very large proportion of octahedral Al. There are two possibilities: (1) there is no pure sepiolite and all analyses are a mixture of sepiolite and palygorskite; or (2) the sepiolites are an anomalous Al-rich sepiolite.

Table 1. Chemical composition (wt.%) of the isolated particles.

	SiO_2	Al_2O_3	MgO	Fe_2O_3	TiO_2	CaO	K_2O		SiO_2	Al_2O_3	MgO	Fe_2O_3	TiO_2	CaO	K_2O
1	70.19	4.07	22.60	2.77		0.36		51	70.38	10.77	16.80	2.00			0.60
2	70.30	3.48	23.34	2.51		0.35		52	63.75	11.34	17.91	2.86	1.00	1.54	1.45
3	69.46	6.26	20.39	3.25		0.48		53	69.74	7.75	19.73	2.00		0.42	0.36
4	70.66	8.80	14.98	5.19				54	70.17	7.75	19.90	1.43	0.33	0.14	0.24
5	67.88	9.71	17.30	4.39		0.73		55	67.60	10.39	16.41	5.00			0.48
6	69.86	5.43	20.66	3.46		0.48		56	67.60	10.01	16.75	4.15		0.70	0.84
7	71.26	8.58	16.35	3.81				57	61.83	10.58	20.06	3.29	4.17		
8	74.44	7.08	15.84	2.64				58	64.82	3.17	19.07	2.29	3.17		1.33
9	73.28	5.94	17.64	3.12				59	65.03	8.50	20.56	5.00	0.83		
10	76.28	8.97	15.35					60	66.10	6.99	23.05	3.86			
11	71.14	4.29	22.26	2.31				61	71.45	11.34	12.60	3.29			0.48
12	72.26	10.59	13.95	3.21				62	72.52	10.96	7.30	1.90	0.33	0.56	0.60
13	69.73	13.45	13.61	3.21				63	62.47	8.88	17.58	0.37	5.00	1.68	
14	70.74	12.08	14.23	2.94				64	70.60	9.64	19.07	0.71			
15	71.27	11.17	13.97	3.59				65	68.24	11.71	14.43	5.58			
16	72.23	10.10	15.25	2.43				66	71.45	10.58	13.26	4.00	0.67		
17	71.45	11.73	13.58	3.23				67	66.75	12.09	11.20	2.72			
18	71.03	11.89	13.88	3.20				68	65.68	13.04	19.90	1.43			
19	71.15	10.74	15.05	3.05				69	68.89	5.29	24.21	1.57			
20	71.66	7.52	17.77	2.89		0.17		70	68.24	4.91	24.71	1.00	0.33	0.07	0.04
21	70.71	6.24	19.44	2.83		0.78		71	65.68	4.53	25.87	3.00	0.33	0.56	
22	72.15	6.57	15.96			3.51		72	66.96	4.72	25.53	2.00		0.84	
23	72.71	8.66	11.05	6.68				73	67.60	6.61	21.55	3.29	0.50	0.28	0.36
24	72.05	4.05	19.25	2.56		0.18	1.91	74	65.03	6.24	24.54	3.00	1.00		
25	73.23	5.39	17.51	3.62				75	67.17	7.56	22.22	1.14	1.00	0.28	0.72
26	69.76	5.09	16.46	2.76			5.69	76	60.97	8.12	25.53	1.29	2.17	0.84	1.08
27	70.3	6.65	18.16	2.75			1.96	77	69.74	8.50	16.91	2.00		0.98	1.93
28	68.75	4.78	22.7	2.18			1.49	78	57.12	10.20	25.87	4.72		1.26	0.84
29	73.46	8.48	14.95	2.64		0.47		79	71.88	9.64	2.82	0.14			
30	71.59	8.68	15.63	3.52				80	65.68	10.96	21.22	1.14		0.10	0.13
31	70.42	13.68	11.09	3.94				81	69.10	10.96	16.75	2.72		0.08	
32	72.08	6.71	21.21					82	66.96	10.58	16.75	2.90		1.26	0.36
33	70.18	10.18	19.64					83	67.17	11.71	17.91	1.43	1.17	0.28	0.36
34	73.46	8.31	18.23					84	65.25	11.71	18.90	1.57	1.83	0.13	
35	69.11	5.33	20.66	3.75			0.81	85	56.26	13.04	20.73	5.15	2.17	0.98	1.81
36	71.18	10.00	13.16	5.12		0.53		86	56.05	11.90	21.22	4.86	3.17	1.54	1.20
37	68.69	4.98	23.53	2.05		0.16	0.55	87	71.24	10.01	13.10	4.15	1.00	0.42	0.36
38	69.49	7.41	18.63	3.93				88	72.52	8.69	12.27	4.00	1.67	0.28	0.48
39	69.53	5.85	21.23	2.69		0.70		89	57.33	9.45	25.04		1.67	2.52	3.85
40	73.73	4.32	19.98	1.97				90	59.04	9.26	23.88			3.50	4.46
41	70.22	6.00	21.27	2.51				91	66.10	3.97	27.19	2.43			0.60
42	70.37	4.89	21.81	2.93				92	71.45	7.94	17.08	2.57	0.33	0.42	
43	69.72	5.45	22.8	1.96				93	72.59	8.12	17.24	1.72			
44	69.02	5.82	21.44	3.37				94	55.41	5.67	19.57	3.86		3.92	3.73
45	66.32	7.18	19.90	3.15	1.83	0.98	0.84	95	61.83	6.05	21.89		4.00	2.66	3.37
46	68.89	7.75	21.72	1.72				96	72.52	8.50	15.25	3.15	0.67		
47	59.69	6.05	25.53	8.86				97	69.53	9.26	15.92	3.43	0.83	0.42	0.60
48	63.32	6.42	24.21	6.00				98	67.40	5.48	21.55	1.86	2.50	0.98	0.36
49	66.10	10.58	18.90	4.43				99	70.38	6.80	17.91	3.00	0.83	0.84	0.24
50	65.80	8.50	18.90	5.15		0.84	0.72								

DISCUSSION AND CONCLUSIONS

Sepiolite is a Mg silicate with negligible isomorphic substitution that has eight possible octahedral positions per half unit-cell, all of them occupied by Mg. According to Newman and Brown (1987) the total munber of octahedral cations ranges from 7.01 to 8.01, and is close to 8 according to Galán and Carretero (1999) who confirmed that both tetrahedral and octahedral substitutions are negligible and cannot be detected by the EDX technique. Nevertheless, if the structural formulae from all of the Allou Kagne analyses are calculated as sepiolite, the number of octahedral cations ranges from 3.12 and 8.04 and the octahedral Mg number varies from 1.73 to 7.09 (4.81 on average) (Table 3), which means that most analyses have a number of octahedral cations and Mg values which are

Table 2. Crystallo-chemical formulae calculated on basis of 21 oxygens per half unit-cell (as palygorskite). Formulae have been ordered according to their content of octahedral cations.

	Si	^{IV}Al	^{VI}Al	Fe^{3+}	Mg	Ti	ΣO	Ca	K		Si	^{IV}Al	^{VI}Al	Fe^{3+}	Mg	Ti	ΣO	Ca	K
11	8.05		0.29	0.10	1.88		2.27			55	7.72	0.28	1.12	0.43	2.79		4.34		0.07
22	8.17		0.88		2.69		3.57	0.43		52	7.37	0.63	0.92	0.25	3.09	0.09	4.35	0.19	0.21
36	8.04		1.33	0.04	2.21		3.58	0.06		5	7.73	0.27	1.03	0.38	2.94		4.35	0.09	
23	8.22		1.15	0.57	1.86		3.58			21	8.01		0.83	0.24	3.28		4.35	0.09	
29	8.35		0.98	0.26	2.40		3.64	0.02		38	7.89	0.11	0.88	0.34	3.15		4.37		
10	8.37		1.16		2.51		3.67			53	7.89	0.11	0.92	0.17	3.33		4.42	0.05	0.05
88	8.17		1.15	0.34	2.06	0.14	3.69	0.03	0.07	64	7.91	0.09	1.18	0.06	3.18		4.42		
54	7.92	0.08	0.23	0.12	3.35	0.03	3.73	0.02	0.03	32	8.07		0.88		3.54		4.42		
62	8.14		1.45	0.23	2.03	0.03	3.74	0.07	0.09	45	7.62	0.38	0.59	0.27	3.41	0.16	4.43	0.12	0.12
26	8.05		0.69	0.24	2.83		3.76		1.27	58	7.43	0.57	0.73	0.20	3.26	0.27	4.46		0.19
8	8.32		0.93	0.22	2.64		3.79			50	7.60	0.40	0.76	0.45	3.25		4.46	0.10	0.11
61	8.04		1.50	0.28	2.11		3.89		0.07	3	7.89	0.11	0.73	0.28	3.45		4.46	0.06	
31	7.91	0.09	1.72	0.33	1.86		3.91			35	7.90	0.10	0.62	0.32	3.52		4.46		0.18
87	8.02		1.33	0.35	2.20	0.08	3.96	0.05	0.05	33	7.85	0.15	1.19		3.28		4.47		
25	8.25		0.72	0.31	2.94		3.97			6	7.94	0.06	0.67	0.30	3.50		4.47	0.06	
95	7.29	0.71	0.13		3.85		3.98	0.34	0.51	39	7.90	0.10	0.68	0.23	3.59		4.50	0.09	
12	8.09		1.40	0.27	2.33		4.00			67	7.55	0.45	1.16	0.23	3.13		4.52		
96	8.13		1.12	0.27	2.55	0.06	4.00			49	7.54	0.46	0.96	0.38	3.21		4.55		
9	8.23		0.79	0.26	2.95		4.00			41	7.95	0.05	0.75	0.21	3.59		4.55		
66	8.03		1.40	0.34	2.22	0.06	4.02			90	7.02	0.98	0.32		4.23		4.55	0.45	0.68
24	8.18		0.54	0.22	3.26		4.02	0.02	0.42	28	7.86	0.14	0.50	0.19	3.87		4.56		0.33
30	8.06		1.15	0.30	2.62		4.07			85	6.65	1.35	0.47	0.46	3.65		4.58	0.12	0.27
16	8.08		1.33	0.20	2.54		4.07			73	7.71	0.29	0.60	0.28	3.67	0.04	4.59	0.03	0.05
93	8.15		1.07	0.14	2.87		4.08			42	7.98	0.02	0.65	0.25	3.69		4.59		
40	8.28		0.57	0.17	3.34		4.08			44	7.86	0.14	0.64	0.32	3.64		4.60		
17	8.00		1.55	0.27	2.27		4.09			1	7.98	0.02	0.53	0.24	3.83		4.60	0.04	
34	8.17		1.09		3.02		4.11			75	7.65	0.35	0.66	0.10	3.77	0.09	4.62	0.03	0.11
18	7.96	0.04	1.53	0.27	2.32		4.12			2	7.99	0.01	0.46	0.21	3.95		4.62	0.04	
15	8.00		1.48	0.30	2.34		4.12			46	7.79	0.21	0.82	0.15	3.66		4.63		
77	7.95	0.05	1.09	0.17	2.87		4.13	0.12	0.28	68	7.43	0.57	1.17	0.12	3.35		4.64		
4	8.00	0.06	1.17	0.44	2.53		4.14			80	7.47	0.53	0.94	0.10	3.60		4.64	0.07	0.09
13	7.82	0.18	1.60	0.27	2.28		4.15			59	7.48	0.52	0.63	0.43	3.52	0.07	4.65		
14	7.93	0.07	1.53	0.25	2.38		4.16			43	7.90	0.10	0.63	0.17	3.86		4.66		
92	8.06		1.05	0.22	2.87	0.03	4.17	0.05		57	7.12	0.88	0.56	0.29	3.45	0.36	4.66		
97	7.89	0.11	1.13	0.29	2.69	0.07	4.18	0.05	0.09	98	7.70	0.30	0.44	0.16	3.86	0.22	4.68	0.12	0.05
19	7.98	0.02	1.40	0.26	2.52		4.18			37	7.83	0.17	0.50	0.18	4.00		4.68	0.02	0.12
27	8.00		0.89	0.24	3.08		4.21		0.43	70	7.72	0.28	0.38	0.09	4.19	0.03	4.69	0.07	0.04
7	8.03		1.14	0.32	2.75		4.21			86	6.63	1.37	0.29	0.43	3.74	0.28	4.74	0.20	0.18
20	8.07		1.00	0.24	2.98		4.22	0.02		89	6.83	1.17	0.16		4.44	0.15	4.75	0.32	0.59
51	7.93	0.07	1.36	0.17	2.70		4.23		0.09	69	7.82	0.18	0.53	0.13	4.10		4.76		
79	8.03		1.27	0.14	2.82		4.23			60	7.57	0.43	0.51	0.33	3.94		4.78		
65	7.75	0.25	1.32	0.48	2.44		4.24			72	7.66	0.34	0.30	0.17	4.36		4.83	0.10	
99	7.98	0.02	0.89	0.26	3.03	0.07	4.25	0.10	0.03	74	7.48	0.52	0.33	0.26	4.21	0.09	4.89		
82	7.65	0.35	1.07	0.36	2.85		4.28	0.15	0.05	71	7.56	0.44	0.18	0.26	4.44	0.03	4.91	0.07	
56	7.72	0.28	1.07	0.36	2.85		4.28	0.09	0.12	76	7.09	0.91	0.20	0.11	4.42	0.19	4.92	0.10	0.16
94	7.23	0.77	0.10	0.38	3.81		4.29	0.55	0.62	48	7.35	0.65	0.23	0.52	4.19		4.94		
83	7.60	0.40	1.16	0.12	3.02		4.30	0.03	0.05	91	7.59	0.41	0.13	0.21	4.65		4.99		0.09
81	7.80	0.20	1.26	0.23	2.82		4.31	0.05		78	6.74	1.26	0.16	0.42	4.55		5.13	0.16	0.13
63	7.25	0.75	0.46	0.37	3.04	0.44	4.31	0.21		47	7.04	0.84		0.79	4.49		5.28		
84	7.42	0.58	0.99	0.13	3.20		4.32	0.09											

too low for sepiolite. Only 14 of the 99 structural formulae obtained as sepiolite have >6 octahedral Mg atoms per half unit-cell. Taking into account the values reported by Newman and Brown (1987), only 1 of the 99 structural formulae calculated in this work could be considered unequivocally as sepiolite. Furthermore, this sepiolite would have a vacant position per half unit-cell.

On the other hand, palygorskite can display greater compositional variations than sepiolite. Galán and Carretero (1999) confirmed that palygorskite contains mainly Mg, Al and Fe with an $R2/R3$ ratio close to 1. On average, four of every five octahedral palygorskite positions are occupied. According to Newman and Brown (1987), the sum of octahedral cations lies between 3.76 and 4.64, with a mean value of 4.00. García Romero *et al.* (2004) reported a very Mg-rich palygorskite that has 4.36 octahedral cations per half unit-cell. They studied a very large number of samples

Table 3. Crystallo-chemical formulae calculated on the basis of 32 oxygens per half unit-cell (as sepiolite). The formulae have been ordered according to their Mg content.

	Si	^{IV}Al	^{VI}Al	Fe^{3+}	Mg	Ti	ΣO	Ca	K		Si	^{IV}Al	^{VI}Al	Fe^{3+}	Mg	Ti	ΣO	Ca	K
17	12.19		1.18	0.21	1.73		3.12			49	11.49	0.51	1.66	0.58	4.90		7.14		
13	11.92	0.08	1.24	0.21	1.73		3.18			50	11.58	0.42	1.34	0.68	4.95		6.97	0.16	0.16
15	12.18		1.13	0.23	1.78		3.14			58	11.32	0.68	1.30	0.30	4.96	0.42	6.98		0.30
19	12.16		1.08	0.20	1.92		3.20			24	12.47		0.83	0.33	4.97		6.13	0.03	0.64
31	12.05		2.76	0.51	2.83		6.10			33	11.97	0.03	2.02		4.99		7.01		
23	12.53		1.76	0.87	2.84		5.47			21	12.20		1.27	0.37	5.00		6.64	0.14	
62	12.41		2.21	0.35	3.09	0.04	5.69	0.10	0.13	53	12.03		1.57	0.26	5.07		6.90	0.08	0.08
88	12.45		1.76	0.52	3.14	0.22	5.64	0.05	0.11	40	12.61		0.87	0.25	5.09		6.21		
61	12.25		2.29	0.42	3.22		5.93	0.15	0.11	54	12.07		1.57	0.18	5.10	0.04	6.89	0.03	0.05
87	12.22		2.02	0.54	3.35	0.13	6.04	0.08	0.08	68	11.32	0.68	1.97	0.19	5.11		7.27		
36	12.25		2.03	0.66	3.37		6.06	0.10		45	11.60	0.40	1.08	0.41	5.19	0.24	6.92	0.18	0.19
66	12.23		2.14	0.52	3.39	0.09	6.14			57	10.86	1.14	1.05	0.43	5.25	0.21	6.94		
18	12.13		2.39	0.41	3.53		6.33			3	12.03		1.28	0.42	5.26		6.96	0.09	
12	12.32		2.13	0.41	3.55		6.09			6	12.11		1.11	0.45	5.33		6.89	0.09	
14	12.08		2.43	0.38	3.62		6.43			35	12.03		1.09	0.49	5.36		6.94		0.27
65	11.80	0.20	2.19	0.73	3.72		6.64			59	11.39	0.61	1.15	0.66	5.37	0.11	7.29		
29	12.53		1.70	0.34	3.80		5.84	0.09		32	12.29		1.35		5.39		6.74		
10	12.81		1.77		3.84		5.61			41	12.11		1.22	0.33	5.46		7.01		
4	12.19		1.79	0.67	3.85		6.31			39	12.04		1.19	0.35	5.48		7.02	0.13	
16	12.31		2.03	0.31	3.87		6.21			80	11.38	0.62	1.62	0.15	5.48		7.25	0.10	0.13
96	12.39		1.71	0.40	3.88	0.09	6.08			44	11.97	0.03	1.16	0.49	5.54		7.19		
30	12.29		1.76	0.45	4.00		6.21			85	10.13	1.87	0.90	0.70	5.56	0.29	7.45	0.19	0.41
8	12.67		1.42	0.34	4.02		5.78			46	11.87	0.13	1.44	0.22	5.58		7.24		
22	12.45		1.34		4.10		5.44	0.65		73	11.76	0.24	1.12	0.43	5.59	0.07	7.21	0.05	0.08
97	12.02		1.89	0.45	4.10	0.11	6.55	0.08	0.13	98	11.73	0.27	0.86	0.24	5.61	0.33	7.04	0.18	0.08
51	12.08		2.18	0.26	4.11		6.55		0.13	42	12.16		1.00	0.38	5.62		7.00		
7	12.24		1.74	0.49	4.19		6.42			86	10.11	1.89	0.64	0.66	5.70	0.43	7.43	0.30	0.28
55	11.76	0.24	1.89	0.65	4.26		6.80		0.11	11	12.26		0.87	0.30	5.72		6.89		
79	12.24		1.24	0.22	4.29		5.75			75	11.66	0.34	1.21	0.15	5.75	0.13	7.24	0.50	0.16
81	11.88	0.22	2.00	0.35	4.29		6.64	0.08		94	11.00	1.00	1.33	0.58	5.80		7.71	0.83	0.95
26	12.27		1.05	0.37	4.31		5.73		1.94	1	12.16		0.83	0.36	5.83		7.02	0.07	
82	11.65	0.35	1.82	0.54	4.34		6.70	0.23	0.08	95	11.12	0.88	0.40		5.87	0.54	6.81	0.51	0.77
56	11.77	0.23	1.82	0.54	4.34		6.70	0.13	0.19	43	12.04		1.11	0.25	5.88		7.24		
92	12.28		1.61	0.33	4.37	0.04	6.35	0.08		28	11.97	0.03	0.95	0.29	5.89		7.13		0.50
93	12.42		1.63	0.22	4.38		6.23			60	11.54	0.46	0.98	0.51	6.00		7.49		
77	12.11		1.74	0.26	4.38		6.38	0.18	0.43										
5	11.78	0.22	1.77	0.57	4.47		6.81	0.14		2	12.18		0.71	0.33	6.02		7.06	0.07	
25	12.57		1.09	0.47	4.48		6.04			37	11.92	0.08	0.94	0.27	6.10		7.31	0.03	0.18
9	12.55		1.20	0.40	4.50		6.10			69	11.92	0.08	1.00	0.20	6.24		7.44		
20	12.29		1.52	0.37	4.54		6.43	0.03		48	11.20	0.80	0.54	0.80	6.38		7.72		
83	11.58	0.42	1.96	0.19	4.60		6.75	0.05	0.08	70	11.84	0.16	0.84	0.13	6.39	0.04	7.40	0.10	0.05
34	12.45		1.66		4.61		6.27			74	11.40	0.60	0.69	0.40	6.41	0.13	7.63		
99	12.16		1.39	0.39	4.61	0.11	6.50	0.16	0.05	90	10.70	1.30	0.68		6.45		7.13	0.68	1.03
63	11.04	0.96	0.89	0.57	4.63	0.67	6.76	0.32		72	11.68	0.32	0.65	0.26	6.64		7.55	0.16	
27	12.18		1.36	0.36	4.69		6.41		0.66	76	10.80	1.20	0.50	0.17	6.74	0.29	7.70	0.16	0.24
52	11.24	0.76	1.60	0.38	4.70		6.68	0.29	0.33	71	11.52	0.48	0.46	0.40	6.76	0.04	7.66	0.11	
67	11.51	0.49	1.97	0.35	4.77		7.09			89	10.40	1.60	0.42		6.77	0.23	7.42	0.49	0.89
38	12.03		1.51	0.51	4.81		6.83			47	10.72	1.28		1.20	6.84		8.04		
64	12.05		1.94	0.09	4.85		6.88			78	10.27	1.73	0.43	0.64	6.93		8.00	0.24	0.19
84	11.31	0.69	1.70	0.21	4.88	0.24	7.03	0.13		91	11.57	0.43	0.39	0.32	7.09		7.80		0.13

from different localities and verified that in all cases the Al content is less than the Mg content in the octahedral sheet, even though the ratio R^{3+}: Mg is close to 1, due to the presence of Fe^{3+} in most samples. In addition, the number of isomorphic substitutions is considerable. The structural formula of this palygorskite has somewhat more Mg than Al, with a ratio of Mg/Al close to 1.3 and a small proportion of Fe^{3+}. Taking into account the 99 structural formulae calculated on the basis of 21 oxygens per half unit-cell (as palygorskite), it is possible to verify that there are many structural formulae that can correspond to palygorskite but they show a very wide compositional variation, ranging from terms very close to the ideal formula (Al/Mg close to 1) to others which are more magnesic (Table 2).

Calculations of structural formulae should give two groups of results, as mentioned above, those corresponding to palygorskite that will fit to 21 oxygens per half

unit-cell, and those corresponding to sepiolite that will fit better to 32 oxygens. Figures 7 and 8 contain all analyses fitted to both possibilities, palygorskite and sepiolite. Whether octahedral occupancy is taken into account (number and type of cations) or whether tetrahedral content is considered, the plots show a group of continuous points, and in no case do the two groups of analyses separate. Whether the number of Si atoms and the total number of octahedral positions filled are taken into account (Figure 7) and the formulae are fitted as palygorskite, it is possible to find a continuous compositional variation which ranges between the richest in Si and lowest octahedral content, and the smallest Si contents and greater number of octahedral cations. Three groups of analyses can be separated. There are: (1) a certain number of points with an excess of Si (>8 Si per half unit-cell); and (2) another group in which >4.5 octahedral positions are filled, that is to say 'trioctahedral palygorskites'. They may correspond to sepiolite when formulae are fitted to 32 oxygens. (3) A third group (containing the most points) is characterized by a Si content between 7.5 and 8, and between 4 and 4.5 octahedral positions filled. This group of points fits well with Mg-rich palygorskite, as described by Chahi *et al.* (2002) and García-Romero *et al.* (2004). In Figure 7, if points that correspond to formulae fitted as sepiolite are analyzed, a continuous compositional variation can also be found between two terms, those with excess Si (>12 atoms per half unit-cell) and small octahedral content, and those with the smallest Si contents and the greatest number of octahedral cations. It is possible, nevertheless, to verify that there is no point that corresponds to sepiolite, and only a few of the points plotted are in the zone between 11.5 and 12 Si atoms and 7–8 octahedral positions occupied.

Mg *vs.* $R2/R3$ is plotted in Figure 8, fitted both as palygorskite and sepiolite formulae. In both cases, there is a continuous variation between the terms with greater $R2/R3$ ratios and Mg content and those having lesser values of both variables. Most analyses fitted for 21 oxygens are projected in the field of palygorskite (taking into account the bibliographic data mentioned above), that is to say, between 2 and 3.5 atoms of Mg, and $R2/R3$ ranges between 1 and 3.5. However, as can be seen in the formulae fitted as palygorskite, most of the analyses correspond to Mg-rich palygorskite, because they are richer in Mg than ideal palygorskite. In contrast, none of analyses is plotted in the sepiolite field when the formulae are fitted to 32 oxygens. The field of sepiolite is plotted in Figure 7, in agreement with data published by Newman and Brown (1987) and Galán and Carretero (1999). Therefore, a field corresponding to sepiolite is plotted between 7 and 8 Mg and >7 for $R2/R3$. In fact, theoretical sepiolite could not be plotted on this graph because the ratio $R2/R3$ is equal to infinity in the ideal formula, in which all octahedral positions are occupied by Mg, and no R^{3+} cations (Al or Fe^{3+}) are present.

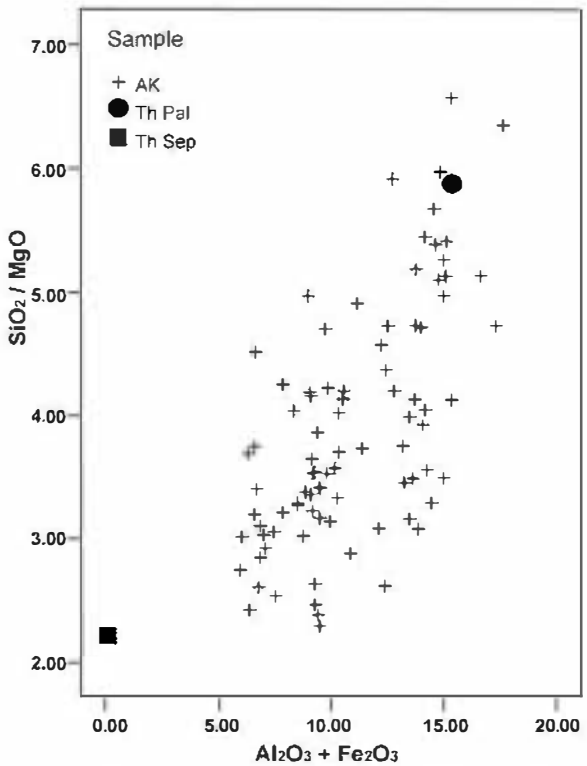

Figure 6. Chemical composition (ratio SiO_2/MgO *vs.* $(Al_2O_3 + Fe_2O_3)$) (%) of the particles analyzed by AEM. Theoretical formulae for palygorskite (●) and sepiolite (■) are also plotted.

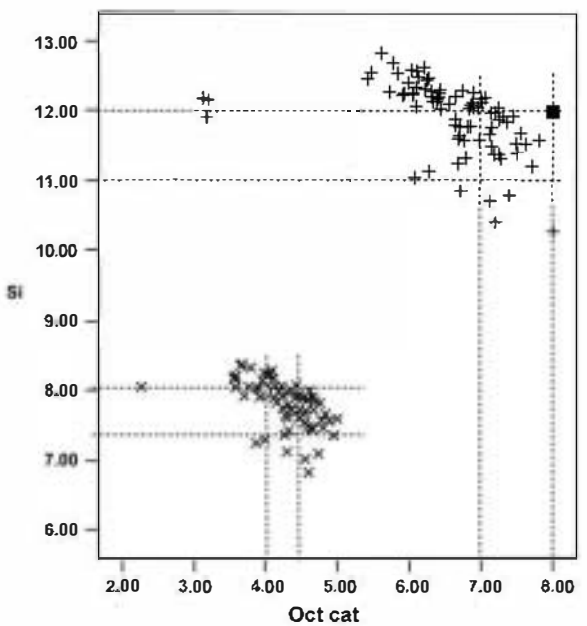

Figure 7. Number of Si atoms *vs.* number of octahedral cations, per half unit-cell, calculated both as palygorskite (×) and as sepiolite (+). Theoretical palygorskite (●) and sepiolite (■) are also plotted.

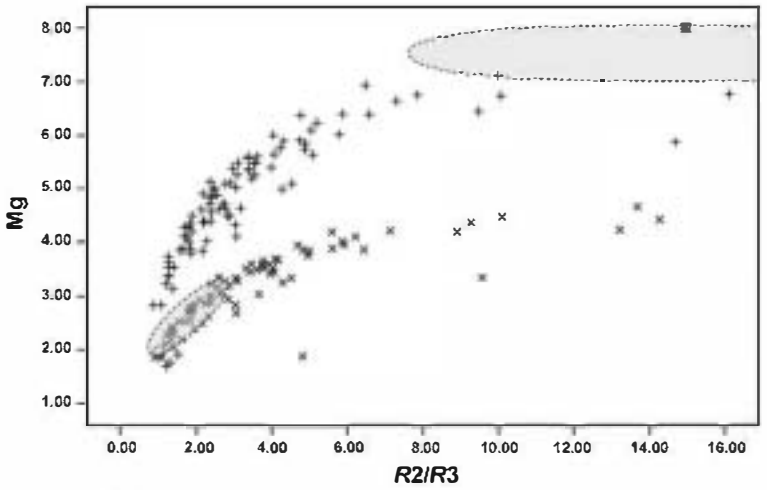

Figure 8. Mg *vs* *R2/R3* (Mg/(Al+Fe^{3+})). All analyses are plotted, and fitted both as palygorskite (×) and as sepiolite (+). Formulae corresponding to theoretical palygorskite (●) and sepiolite (■) are also plotted. The gray fields correspond to areas in which sepiolite could be projected taking into account possible isomorphic substitution after data reported in the literature (see text).

In Figure 8 none of the analyses is plotted in the sepiolite field but as sepiolite was determined by XRD in a proportion between 20–30 %, there should be a similar proportion in the analyzed fibers. All the AEM analyses have been carried out on isolated fibrous particles but, nevertheless, it is not possible to confirm that all of them correspond to pure palygorskite or pure sepiolite. Two possibilities must be considered: (1) sepiolite from Allou Kagne deposit has an important number of isomorphic substitutions and is therefore an Al-rich sepiolite, or (2) analyses actually correspond to fibers of palygorskite and sepiolite together.

It is clear that there are fibers of pure palygorskite and pure sepiolite, as can be seen by SAED (Figure 5a,b), and there are also particles formed by a mixture of sepiolite and palygorskite (Figure 5d). The isolated fibers that can be seen by TEM correspond to aggregates of several fibers of smaller size, and in this case they may be a mixture of crystals of sepiolite and palygorskite with different proportions of crystallites of both minerals. Although the possibility of the mixture of fibers of both minerals can be taken into account, as most of the fibers are monomineralic, then sepiolite must be very rich in Al.

From the data set out above, some genetic considerations can be made. The Allou Kagne sepiolite-palygorskite was generated by sedimentation in an epicontinental marine environment. Sedimentary features of the levels studied have been seen in hand specimens and by SEM, and no evidence of diagenetic processes has been observed. Furthermore, there is evidence of authigenic formation of both sepiolite and palygorskite fibers. Therefore, palygorskite-sepiolite levels are the result of a chemical precipitation and the crystallochemical characteristics of the mineral particles should be a result of chemical composition of the solution. As the aggregates observed by SEM as small bundles are formed by very small numbers of fibers that can be either palygorskite, sepiolite, or both, this indicates the close genetic relationship between them, and epitactic growth may even be possible.

As has already been mentioned, it is not often that sepiolite and palygorskite co-exist in nature. Experimental studies on the stability of fibrous clays show that sepiolite and/or palygorskite occurrences in sedimentary environments indicate saline conditions, with high activity of Si and Mg and high pH (8–10) (Siffert and Wey, 1962; Wollast *et al.*, 1968; La Iglesia, 1977). The formation of sepiolite or palygorskite depends on the availability of Al (Hay and Wiggins, 1980; Singer and Norrish, 1974). In the Allou Kagne deposit, palygorskite and sepiolite appear with X-ray amorphous silica. Direct precipitation of sepiolite and palygorskite from solutions is more favored in the presence of X-ray amorphous silica than with quartz, and it is also favored by small values of log $[a{Al^{3+}}/(a{H^{+}})^3]$ (Birsoy, 2002).

Textural and microtextural features (Figure 4) allow us to propose that fibrous clay minerals of the Allou Kagne deposit were formed by direct precipitation from solution. If both minerals precipitate together from the same solution, so close together that sometimes they comprise a single small bundle, this suggests that they grow at the same time and therefore formation conditions were very restricted, close to the limit of their stability fields. Lower aqueous Al activities favor the non-Al phases (sepiolite) with respect to the Al-containing phases (palygorskite). At lower pH values, palygorskite can be formed by the transformation of the amorphous silica and dioctahedral smectites. At slightly higher pH values, sepiolite, amorphous silica and palygorskite can form from the solution. In silica-poor solutions the formation of sepiolite requires a higher pH than that of palygorskite. Concentrated silica solutions

(log $[aH_4SiO_4]$ > −4.75) but lower Al activities are the most favorable conditions for the direct precipitation of sepiolite from solution (Birsoy, 2002).

The chemical composition of the solution favored the formation of palygorskite rather than sepiolite, due to the presence of reactive Al in the solution with significant values of Mg and Si activity. A wide compositional variation of palygorskites and sepiolites (from palygorskites close to ideal formula to others very rich in Mg or Al) appear as a consequence of temporary variations of the chemical composition of the solution. These compositional variations could be a consequence of cyclical variations in the formation of palygorskite which consumes Al. The variations in the composition of the solutions could also be influenced by the formation of intermediate colloidal phases as ultrafine aluminous colloids. When palygorskite forms, Al activity is reduced, and the new conditions favor the precipitation of sepiolite. Logically, sepiolite precipitation removes Mg from the solution and increases Al activity, and a new cycle begins with new precipitation of palygorskite. Both phases can even form in the same cycle, due to the proximity of the two phases in the stability diagrams, thus allowing the formation of both minerals by point changes in the microchemical conditions.

Palygorskites in calcareous formations are occasionally mixed with smectites. The octahedral composition of smectites and fibrous clays partly overlap. Sepiolite is clearly in the trioctahedral domain but the palygorskite field is both in the dioctahedral domain as well as between the dioctahedral and trioctahedral domains of smectites (Paquet *et al.*, 1987). However, it is clear that smectites mixed with the fibrous clays do not appear in the Allou Kagne deposits, suggesting a relatively more alkaline, siliceous and magnesic environment compared to that which is necessary for the formation of smectite, but not necessarily more saline (Jones and Galán, 1988). The increased evaporation of water, together with an increase in alkali activity and in pH, would favor the formation of mixed-layer kerolite-stevensite. The trioctahedral smectite forms in the same system at higher pH (Khoury *et al.*, 1982). Precipitation of sepiolite and/or palygorskite depended on evaporation, and on rain and fresh-water flows that temporarily changed the pH in some parts of the closed basin. Semi-arid climatic conditions interrupted by humid intervals prevailed, and these did not allow the development of evaporitic facies except for dolomites and/or limestones.

ACKNOWLEDGMENTS

The authors are grateful to Adrian Gómez Herrero of the Centro de Microscopía Electrónica 'Luis Bru (U.C.M.), and to Catherine Doyle for checking and improving the English. The work benefited from helpful comments by Dr Blair Jones and Dr Crawford Elliott. Financial support by CICYT (project CGL2006-09843/BTE) is acknowledged. Additional funding was obtained from Grant 910386 (Universidad Complutense, Grupos de Investigación).

REFERENCES

Akbulut, A. and Kadir, S. (2003) The geology and origin of sepiolite, palygorskite and saponite in Neogene lacustrine sediments of the Serinhisar-Acipayam Basin, Denizly, SW Turkey. *Clays and Clay Minerals*, **51**, 279–292.

Alvarez, A. (1984) Sepiolite properties and uses. Pp. 253–287 in: *Palygorskite-Sepiolite. Occurrences, Genesis and Uses* (A. Singer and E. Galán, editors). Developments in Sedimentology, **37**. Elsevier, Amsterdam.

Bailey, S.W. (1980) Structure of layer silicates. Pp. 1–123 in: *Crystal Structures of Clay Minerals and their X-ray Identification* (G.W. Brindley and G. Brown, editors). Monograph **5**, Mineralogical Society, London.

Birsoy, R. (2002) Formation of sepiolite-palygorskite and related minerals from solution. *Clays and Clay Minerals*, **50**, 736–745.

Bowles, A., Angino, E.A., Hosterman, J.W. and Galle, O.K. (1971) Precipitation of deep-sea palygorskite and sepiolite. *Earth and Planetary Science Letters*, **11**, 324–332.

Bradley, W.F. (1940) The structural scheme of attapulgite. *American Mineralogist*, **25**, 405–411.

Brauner, K. and Preisinger A. (1956) Estruktur und Enstehung des sepiolits. *Tschermaks Mineralogische und Petrographisches Mitteilungen*, **6**, 120–140.

Castillo, A. (1991) Geología de los yacimientos de minerales del grupo paligorskita-sepiolita. Pp. 609–636 in: *Yacimientos minerales, Técnicas de estudio, Tipos, Evolución metalogenética, Exploración* (R. Lunar and R. Oyarzun, editors). Editorial Centro de Estudios ramón Areces, S.A., Spain.

Chahi, A., Fritz, B., Duplay, J., Weber, F. and Lucas, J. (1997) Textural transition and genetic relationship between precursor stevensite and sepiolite in lacustrine sediments (Jbel Rhassoul, Morocco). *Clays and Clay Minerals*, **45**, 378–389.

Chahi, A., Petit, S. and Decarreau, A. (2002) Infrared evidence of dioctahedral-trioctahedral site occupancy in palygorskite. *Clays and Clay Minerals*, **50**, 306–313.

Estéoule-Choux, J. (1984) Palygorskite in the Tertiary deposits of the Armorican Massif. Pp. 75–85 in: *Palygrorskite-Sepiolite. Occurrences, Genesis and Uses* (A. Singer and E. Galán, editors) Developments in Sedimentology, **37**. Elsevier, Amsterdam.

Galán, E. and Carretero, I. (1999) A new approach to compositional limits for sepiolite and palygorskite. *Clays and Clay Minerals*, **47**, 399–409.

Galán, E. and Castillo, A. (1984) Sepiolite-palygorskite in Spanish Tertiary basins: Genetical patterns in continental environments. Pp. 87–124 in: *Palygorskite-Sepiolite. Occurrences, Genesis and Uses* (A. Singer and E. Galán, editors). Developments in Sedimentology, **37**. Elsevier, Amsterdam.

Galán, E. and Ferrero, A. (1982) Palygorskite-sepiolite clays of Lebrija, Southern Spain. *Clays and Clay Minerals*, **30**, 191–199.

Garcia-Romero, E., Suárez Barrios, M. and Bustillo Revuelta, M.A. (2004) Characteristics of a Mg-palygorskite in Miocene rocks (Madrid Basin, Spain). *Clays and Clay Minerals*, **52**, 486–494.

Garcia-Romero, E., Suárez, M., Oyarzun, R., López-García, J.A. and Regueiro, M. (2006) Fault-hosted palygorskite from the Serrata de Níjar deformation zone (SE Spain). *Clays and Clay Minerals*, **54**, 324–332.

Haji-Vassilou, A. and Puffer, J.H. (1975) A macrocrystalline attapulgite-palygorskite ocurrence in calcite veins. *American Mineralogist*, **60**, 328–330.

Hay, R.L. and Wiggins, B. (1980) Pellets, ooids, sepiolite and silica in three calcretes of the southwestern United States.

Sedimentology , **27**, 559–576.

Jones, B.F. and Galán, E. (1988) Sepiolite and palygorskite. Pp. 631–674 in: *Hydrous Phyllosilicates (exclusive of micas)* (S.W. Bailey, editor). Reviews in Mineralogy, **19**. Mineralogical Society of America, Washington, D.C.

Kamineni, D.C., Griffault, L.Y. and Kerrich, R. (1993) Palygorskite from fracture zones in the Eye–Dashwa Lakes granitic pluton, Atikokan, Ontario. *The Canadian Mineralogist*, **31**, 173–183.

Khoury, J.N., Eberl, D.D. and Jones, B.F. (1982) Origin of magnesium clays from the Amargosa Desert, Nevada. *Clays and Clay Minerals*, **30**, 327–336.

La Iglesia, A. (1977) Precipitación por disolución homogénea de silicatos de aluminio y magnesio a temperatura ambiente. Síntesis de la paligorskita. *Estudios Geológicos*, **33** 535–544.

Leguey, S., Martín Rubí, J.A., Casas, J., Marta, J., Cuevas, J., Álvarez, J. and Medina, J.A. (1995) Diagenetic evolution and mineral fabric in sepiolitic materials from the Vicalvaro Deposit (Madrid Basin). Pp. 383–392 in: *Proceedings of the 10th International Clay Conference, Adelaide.*

Lopez-Galindo, A., Ben Aboud, A., Fenoll Hach-Ali, P. and Casas Ruiz, J. (1996) Mineralogical and geochemical characterization of palygorskite from Gabasa (NE Spain). Evidence of a detrital precursor. *Clay Minerals*, **31**, 33–44.

Martín Pozas, J.M., Sánchez Camazano, M. and Martín Vivaldi Martínez, J.L. (1981) La Paligorskita de Tabladillo (Guadalajara). *Boletín Geológico y Minero*. **XCII-V**, 395–402.

Martín Vivaldi, J.L. and Cano, J. (1956) Contribution to the study of sepiolite: II Some considerations regarding the mineralogical formula. Pp: 173–176 in: *Proceedings of the fourth National Conference on Clays and Clay Minerals.* National Academy of Sciences – National Research Council Publication 456, 1956, USA.

Millot, G. (1970) *Geology of Clays: Weathering, Sedimentology, Geochemisty.* Springer Verlag, New York, 430 pp.

Newman, A.C.D. and Brown, G. (1987) The chemical constitution of clays. Pp. 1–128 in: *Chemistry of Clays and Clay Minerals* (A.C.D. Newman, editor). Monograph **6**, The Mineralogical Society, Longman Scientific and Technical, Harlow, Essex, UK.

Paquet, H., Duplay, J., Vallerçon-Blanc, M.M. and Millot, G. (1987) Octahedral compositions of individual particles in smectite-palygorskite and smectite-sepiolite assemblages. Pp. 73–77 in: *Proceedings of the International Clay Conference, Denver*, 1985 (L.G. Schultz, H. Van Olphen and F.A. Mumpton, editors), The Clay Minerals Society, Bloomington, Indiana.

Serna, C., Van Scoyoc, G.E. and Ahlrichs, J.L. (1977) Hydroxyl groups and water in palygorskite. *American Mineralogist*, **62**, 784–792.

Siffert, B. and Wey, R. (1962) Synthèse d'une sépiolite à température ordinaire. *Comptes rendus de l'Academie des sciences, Paris*, **245**, 1460–1463.

Singer, A. (1984) Pedogenic palygorskite in the arid environment. Pp. 169–175 in: *Palygorskite-Sepiolite. Occurrences, Genesis and Uses* (A. Singer and E. Galán, editors). Developments in Sedimentology, **37**. Elsevier, Amsterdam.

Singer, A. and Norrish, K. (1974) Pedogenetic palygorskite. Occurrences in Australia. *American Mineralogist*, **59**, 508–517.

Suárez, M., Robert, M., Elsass, F. and Martín Pozas, J.M. (1994) Evidence of a precursor in the neoformation of palygorskite – New data by analytical electron microscopy. *Clay Minerals*, **29**, 255–264.

Tien, P.L. (1973) Palygorskite from Warren Quarry, Enderby, Leicestershire, England. *Clay Minerals*, **10**, 27–34.

Torres-Ruiz, J., López-Galindo, A., González-López, J.M. and Delgado, A. (1994) Geochemistry of Spanish sepiolite-palygorskite deposits: Genetic considerations based on trace elements and isotopes. *Geochemical Geology*, **112**, 221–245.

Verrecchia, E.P. and Le Coustumer, M.N. (1996) Occurrence and genesis of palygorskite and associated clay minerals in Pleistocene calcrete complex, Sde Boqer, Negev desert, Israel. *Clay Minerals*, **31**, 183–202.

Watts, N.L. (1976) Paleopedogenic palygorskite from the basal Permo-Triassic of northwest Scotland. *American Mineralogist*, **61**, 299–302.

Watts, N.L. (1980) Quaternary pedogenic calcretes from the Kalahari (southern Africa): mineralogy, genesis and diagenesis. *Sedimentology*, **27**, 661–686.

Weaver, C.E. (1984) Origin and geologic implications of the palygorkite of S.E. United States. Pp. 39–58 in: *Palygorskite-Sepiolite. Occurrences, Genesis and Uses* (A. Singer and E. Galán, editors). Developments in Sedimentology, **37**. Elsevier, Amsterdam.

Wollast, R., Mackenzie, F.T. and Bricker, O. (1968) Experimental precipitation and genesis of sepiolite at earth-surface conditions. *American Mineralogist*, **53**, 1645–1662.

Yaalon, D.M and Wieder, M. (1976) Pedogenetic palygorskite in some arid brown (calciothid) soils of Israel. *Clay Minerals*, **11**, 73–79.

Zaaboub, N., Abdeljapouad, S. and López Galindo, A. (2005) Origin of fibrous clays in Tunisian Paleogene continental deposits. *Journal of African Earth Sciences*, **43**, 491–504.